water

MDPI

Article

Nitrate and/or Nitric Acid Formation in the Presence of Different Radical Scavengers during Ozonation of Water Samples; Are Scavengers Effective?

Ulker D. Keris-Sen [1] and Taner Yonar [2,*]

[1] Institute of Earth and Marine Sciences, Gebze Technical University, Gebze 41400, Kocaeli, Turkey; udkeris@gtu.edu.tr
[2] Department of Environmental Engineering, Bursa Uludag University, Nilufer 16059, Bursa, Turkey
* Correspondence: yonar@uludag.edu.tr

Abstract: In this study, we investigated the effect of different radical scavengers on the nitrate and/or nitric acid (NO_3^- and/or HNO_3) formation chain in liquid while the dielectric barrier discharge plasma system (DBD) was used for ozone (O_3) generation. The effects of the excess concentration of each scavenger were studied individually. In addition, ultrapure water (UPW), tap water, and surface water samples were examined in the same condition. Due to the absence of scavengers in the UPW, we expected the highest NO_3^- formation in this experiment because all active species produced by the DBD system should have formed NO_3^-. However, the obtained results were unexpected; the highest NO_3^- formation was obtained in the tap water at 385 ± 4.6 mg/L. The results can be explained by some compounds in tap water acting as a trap for radicals involved in chain reactions that form NO_3^- and/or HNO_3. The second highest result was obtained in the sodium hydroxide solution as 371 ± 4.9 mg/L, since the OH^- ions accelerated the decomposition of O_3 to its intermediates such as hydroperoxide (HO_2^-), ozonide (O_3^-), and hydroxyl radical ($OH^\bullet$), and, by increasing radicals in the liquid, more chain reactions can be promoted that lead to the formation of NO_3^- and/or HNO_3. On the other hand, the quenching of radicals by scavengers such as carbonate ion and phosphoric acid and/or the long-term stabilization of O_3 as O_3 negatively affected the chain reactions that generate NO_3^- and/or HNO_3.

Keywords: ozonation; DBD; nitrate and/or nitric acid formation; radical scavengers

Citation: Keris-Sen, U.D.; Yonar, T. Nitrate and/or Nitric Acid Formation in the Presence of Different Radical Scavengers during Ozonation of Water Samples; Are Scavengers Effective?. *Water* **2023**, *15*, 1840. https://doi.org/10.3390/w15101840

Academic Editors: Maria Cristina Collivignarelli, Alessandro Abbà and Chiara Milanese

Received: 10 March 2023
Revised: 29 April 2023
Accepted: 6 May 2023
Published: 11 May 2023

1. Introduction

Nitrogen (N) is one of the valuable substances for the living cell, its main source is the atmosphere and about 78% of the air is inert nitrogen gas (N_2). The inert form of N_2 is converted to the reactive form as ammonia by the Haber–Bosch process (H-B) and then as nitric acid by the Ostwald process. On the other hand, inert N_2 in the air can be converted to reactive nitrogen species (RNS) by non-thermal plasma systems (NTP) which provided reactive oxygen species (ROS). In the plasma field, chain reactions occur between high-voltage electrons (e*) and gas molecules, thus the gas molecules split into their reactive atomic forms such as oxygen atoms ($O^\bullet$) and nitrogen atoms ($N^\bullet$) via Equations (1) and (2) [1,2].

$$e^* + O_2 \rightarrow 2O^\bullet + e^- \quad (1)$$

$$e^* + N_2 \rightarrow N^\bullet + N^\bullet + e \quad (2)$$

Different kinds of active species are formed/deformed incessantly, such as an $O^\bullet$ reacts with other O_2 to generate ozone (O_3) Equation (3) [1], or with other pathways provided to generate superoxide ($^\bullet O_2^-$) and peroxide ($^\bullet O_2^{2-}$).

$$O^\bullet + O_2 \rightarrow O_3 \quad (3)$$

Nitric oxide ($NO^{\bullet}$) is formed by the reaction between $N^{\bullet}$ and $O^{\bullet}$ (Equation (4)) or can be formed as an intermediate of N_2O_2 from the reaction of $O^{\bullet}$ or O_3 with N_2O (Equation (5)) [3,4]. Then, $NO^{\bullet}$ can be oxidized to nitrogen dioxide ($NO_2^{\bullet}$) by O_3 (Equation (6)) [3].

$$N^{\bullet} + O^{\bullet} \rightarrow NO^{\bullet} \quad (4)$$

$$O^{\bullet} + N_2O \leftrightharpoons N_2O_2 \leftrightharpoons 2NO^{\bullet} \quad (5)$$

$$NO^{\bullet} + O_3 \leftrightharpoons NO_2^{\bullet} + O_2 \quad (6)$$

Nitrogen trioxide ($NO_3^{\bullet}$) can occur by a reaction between $NO_2^{\bullet}$ and O_3, or rather $O^{\bullet}$ (Equations (7) and (8)) [5]. The instantaneous reaction between $NO_2^{\bullet}$ and $NO_3^{\bullet}$ provides the formation of dinitrogen pentoxide (N_2O_5) (Equation (9)) [5].

$$O_2^{\bullet} + O_3 \rightarrow NO_3^{\bullet} + O_2 \quad (7)$$

$$NO_2^{\bullet} + O^{\bullet} \rightarrow NO_3^{\bullet} \quad (8)$$

$$NO_2^{\bullet} + NO_3^{\bullet} \rightleftharpoons N_2O_5 \quad (9)$$

Some of the active species can be transferred to the liquid phase without quenching as a function of gas flow [3,6,7]. The interaction between the active species and water molecules can result in the formation of different species such as peroxynitrite ($ONOO^-$) which can be formed by a reaction between $NO^{\bullet}$ and $^{\bullet}O_2^-$ (Equation (10)) [3]. In the liquid phase, peroxynitrous acid (ONOOH) is generated by $ONOO^-$ and H^+ (Equation (11)) [3]. ONOOH is an isomer of HNO_3 (Equation (12)) [3].

On the other hand, cyclic O_3 formation initiates in the liquid phase and, its intermediates such as hydroxyl radical ($OH^{\bullet}$), hydroperoxyl radicals ($^{\bullet}HO_2$), and hydrogen peroxide (H_2O_2) [8], can be involved in HNO_3 formation in the liquid (Equations (13) and (14)) [3]. NO_3^- can be formed by dissociating ONOOH in the water (Equation (15)) [3].

$$NO^{\bullet} + {}^{\bullet}O_2^- \rightarrow ONOO^- \quad (10)$$

$$ONOO^- + H^+ \rightleftharpoons ONOOH \quad (11)$$

$$HOONO \rightleftharpoons HNO_3 \quad (12)$$

$$NO^{\bullet} + OH^{\bullet} \rightarrow HNO_2 \quad (13)$$

$$HNO_2 + H_2O_2 \rightarrow ONOOH + H_2O \quad (14)$$

$$ONOOH \rightarrow NO_3^- + H^+ \quad (15)$$

Except for the above reactions, there are dozens of possible reaction mechanisms that have been reported in previous studies [3,5–7,9,10].

In addition, the active species can react with any substance in the water, such as scavenger ions, molecules, and/or living cells [3,6,9]. The presence and concentration of scavengers affect the half-life of the active species [9].

In addition, the oxidation effect of the ROS and RNS in the liquid has been emphasized in many previous studies, and their interaction with the water matrix and/or each other has been the focus of several studies with increasing interest, over the last decade [3,6,11].

Oehmigen et al. investigated the disinfection effect of the RNS/ROS on *E. coli.* They stated that the interaction of radicals with water provided the formation of HNO_3 which caused acidification of water and increased the degree of disinfection. HNO_2 formation in the water leads to part of the HNO_3 formation; moreover, the oxidation tendency of the NO_2^- to NO_3^- and/or ONOOH formation can also be improved for HNO_3 formation [3]. The radical formation in the liquid phase and their active role of them in the oxidation and biocidal effects were examined on two different targets, *E. coli* and the phenol by Lukes et al. [6]. They proved that $NO^\bullet$ and $NO_2^\bullet$ radicals and the NO^+ ions are formed at the gas–liquid interface through the intermediates of phenol and, they showed that as a function of pH, the formation of the phenol byproducts is changed which was evidence that the radicals are influenced by pH [6].

Takahashi et al. investigated the effect of feed gas composition on RNS/ROS formation by a different type of plasma source; they stated that N_2O_5 was effective for the formation of HNO_3, and production was increased as a function of specific energy. They also achieved the NO_3^- in water when using it without O_2 in the feed gas by pulsed discharge, they explained it by the possible long life acting to produce NO_3^- in off-gas sparging above the water [7].

One of the previous studies focusing on the production of HNO_3 by pulsed high voltage discharge showed that pH is the most important parameter; increasing the pH of the solution reduces the degree of conversion of NO_2^- to NO_3^- and consequently, HNO_3 formation efficiency is decreased [4].

Moreover, Buendia et al. investigated the effect of $NaHCO_3$ alkalinity on NO_3^- formation by using DBD above the water surface. They reported that the increase in initial sodium bicarbonate concentration caused a decrease in the rate of NO_3^- formation [12].

Consequently, different types of plasma chemical reactions can be triggered depending on the discharge's type, energy, and chemical composition of the environment in which it operates, encompassing both gaseous and liquid phases. These discharges can give rise to a variety of species at the gas–liquid interface, which can penetrate or dissolve into the liquid and instigate chemical processes [6,7,13]. Therefore, we do not believe comparing previous studies with each other is a correct approach. However, it was believed that the relationship between the scavengers in the liquid phase and the active species could be defined only if the plasma variables were kept constant, and the current study was carried out with this approach. In this study, the DBD system and environmental circumstances were kept constant for all experiments. We examined the most common radical scavenger ions found in typical natural water sources with their excess concentrations to better compare their scavenging activity on NO_3^- and/or HNO_3 formation. In addition, tap and surface water samples were also assessed in terms of their radical scavenging effect on NO_3^- and/or HNO_3 formation when the samples were treated with the system.

2. Materials and Methods

2.1. Chemicals and Water Samples

The potassium iodide (KI), sodium thiosulfate ($Na_2S_2O_3$), sodium nitrate ($NaNO_3$), sodium bicarbonate ($NaHCO_3$), sodium carbonate (Na_2CO_3), sodium chloride (NaCl), calcium dichloride ($CaCl_2$), sodium hydroxide (NaOH), Ceric sulfate tetrahydrate ($Ce(SO_4)_2{\cdot}4H_2O$), and hydrogen peroxide (H_2O_2 purity, 36.5%) used in the experiments were analytical grade and obtained from Sigma Aldrich. The nitric acid (HNO_3) (purity 65%) and sulfuric acid (H_2SO_4) (purity, 98%), ceric sulfate was purchased from Merck. The tap water sample was obtained from the local water network system, while the surface water was sampled from 10–15 cm under the surface of the Karadere River in Yalova, NW Turkey. The surface water samples obtained from the field were transported in 500 mL polyethylene containers to the laboratory at −4 °C with a portable sample carrying bag. After the samples were brought to the laboratory, they were stored at −18 °C and analyzed within 2 days. The surface water sample was labeled as KSW. The ultra-purified water (as labeled UPW) was obtained from a Millipore Milli-Q water purification system.

2.2. Analytical Methods

Elemental analysis of tap water and surface water samples was measured using an Inductively Coupled Plasma Optical Emission Spectroscopy (ICP-OES Optima 7000DV). Details on ICP-OES instrumental operating conditions and measuring parameters used are given in Table 1.

Table 1. ICP-OES operating conditions.

Parameter	Operation Conditions
RF power, W	1450
Sample uptake rate, mL/min	1.5
Nebulization gas flow rate, L/min	0.45
Auxiliary gas flow rate, L/min	0.2
Plasma flow rate, L/min	15
Sample flow rate, L/min	1.5
Nebulizer	Cross Flow
Spray chamber	Scott
Torch configuration	Radial (Ca, Mg, Na), Axial (Fe, Zn, Ba, K, Cu)
Elements, wavelengths (nm)	Fe (259.939), Zn (206.200), Ba (455.403), Mg (280.271), Ca (393.366), K (766.490), Na (589.592), Cu (327,393)

NO_3^- and/or HNO_3 analysis was performed by measuring nitrate ion concentration in the samples using an ion chromatograph (IC-Shimadzu Prominence series) equipped with a Shim-pack IC-SA2 column (250 mm L. × 4.0 mm I.D) and a conductivity detector. The mobile phase was a mixture of $NaHCO_3$ (12 mM), Na_2HCO_3 (0.6 mM), and UPW. The flow rate is 1 mL/min, and the oven temperature is 30 °C. Before the analysis, the samples were filtered through 0.45 µm syringe filters. The injection volume was set as 20 µL. A standard ion solution (Shimadzu Ion mix) was used for preparing the calibration curve.

The ozone generation capacity of the generator was determined by iodometric titration according to Standard Methods 2350-E [14].

Total organic carbon (TOC), total carbon (TC), and inorganic carbon (IC) concentrations were measured using a TOC-Analyzer (Shimadzu, TOC-L, Kyoto, Japan).

Residual hydrogen peroxide was measured by modifying the ceric sulfate titration method [15]. Since the residual hydrogen peroxide was in very small amounts in our experiments, different from the original method, 0.01 N ceric sulfate solution was used in the analysis. The modified version limit of the detection was 0.11 mM H_2O_2.

2.3. Experimental Set-Up

The experimental set-up used in the experiment is given in Figure 1. In all experiments performed with a bench-top DBD, the transformer was 4 kV, 13.7 kHz, the plate to plate electrodes size was 14 mm × 5 mm × 8 mm covered by the ceramic barrier, the gap distance of the electrode was 1.1 mm, and the DBD was in the glass hermetical rectangular parallelepiped. The transformers and electrodes used in our study were produced specially for us by Ulus Electronic in Kocaeli, Turkey. The glass hermetical rectangular parallelepiped was assembled by us in our laboratory.

The reactor outlet gas was delivered through a glass diffuser to a glass cylindrical water column (50 cm in length and 6 cm diameter) by bubbling at a flow rate of 3 L/min, and the reactor contained 200 mL of liquid. The reactor was produced specially for us by Dilex in İstanbul, Turkey. The exit gas from the reaction column was passed through two serial-connected Drechsel bottles (exhaust gas bottles) (Dräger) filled with 500 mL of 2% KI solution to capture and measure ozone and radicals. In all experiments, the ambient air was used as feed gas to the generator at 3 L/min.

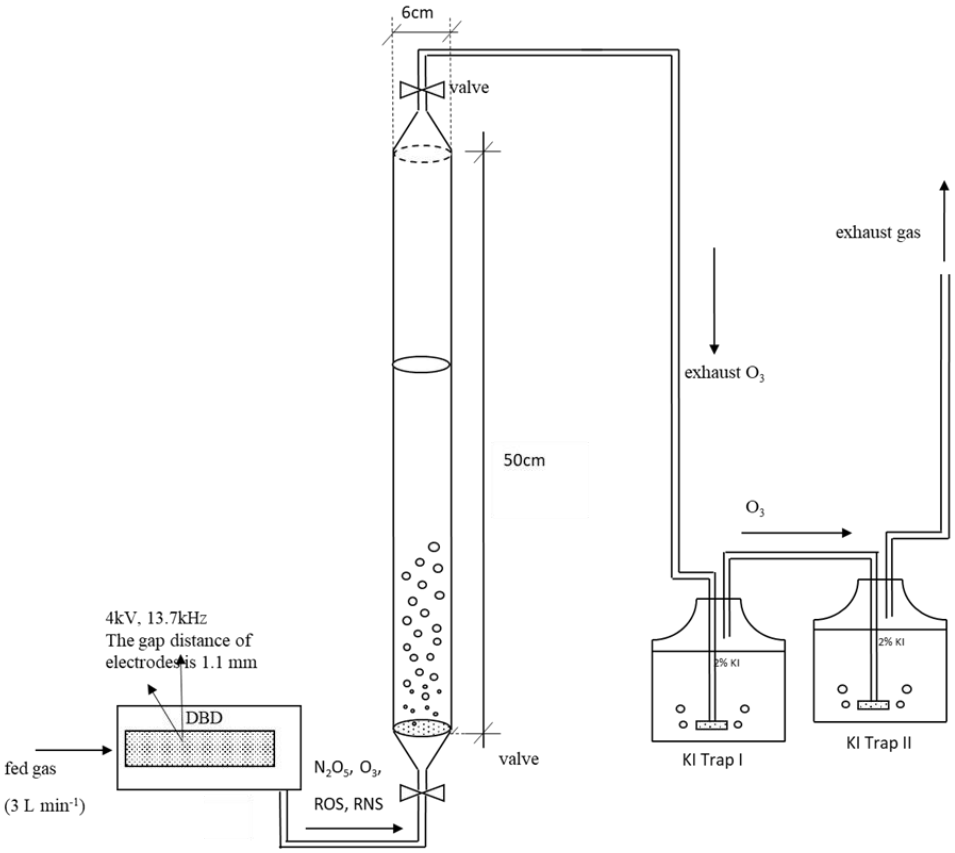

Figure 1. A schematic diagram of the set-up used for all experiments in the current work.

2.4. Determination of the Effect of the Water Matrix on NO_3^- and/or HNO_3 Formation

To determine the effect of the pH, a 5 mM NaOH solution, a 0.01 N HCl solution, and a 0.01 N H_3PO_4 solution were used. The effect of the inorganic carbon alkalinity and species was examined using a $NaHCO_3$ solution and an Na_2CO_3 solution was prepared; both solutions have the same alkalinity of 500 mg/L as $CaCO_3$. The effect of the ionic strength of the water was investigated with NaCl and $CaCl_2$ solutions with the same ionic strength (μ) as 0.7 M. In addition, tap and surface water samples containing various radical scavengers in low concentrations were also examined. A partial analysis of tap water and KSW is given in Table 2. All solutions were examined separately, and the experiments were performed in triple replicate.

Table 2. All solutions were examined separately, and the experiments were performed in triple replicate.

Parameter	KSW	Tap Water	Parameter	KSW	Tap Water
Element	mg/L	mg/L	pH	7.40	8.50
Total Fe	0.002	0.005	Alkalinity (mg/L as $CaCO_3$)	170 (±5.15)	110 (±5.15)
Total Zn	0.004	0.019			
Total Ba	0.003	0.011	Hardness (mg/L as $CaCO_3$)	125 (±10.2)	190 (±10.2)
Total Mg	10.668	13.830			
Total Ca	106.350	39.760	Conductivity (μS/cm)	565	230
Total K	0.511	1.274			

Table 2. *Cont.*

Parameter	KSW	Tap Water	Parameter	KSW	Tap Water
Total Na	12.959	9.095	TC (mg/L)	114 (±0.5)	60.5 (±0.5)
Total Cu	0.002	0.007	TOC (mg/L)	10 (±0.5)	0.00
Br^-	0.000	0.007	Inorganic carbon (mg/L)	100 (±0.5)	60 (±0.5)
Cl^-	5.800	7.900			
NO_3^-	2.413	0.655			
PO_4^{3-}	0.920	0.420	ICP analysis standard deviation is ± 0.005 mg/L,		
SO_4^{2-}	14.400	8.810			

2.5. Statistical Analysis

Linear regression and one-way Welch's analysis of variance (ANOVA) were performed for the statistical assessment of NO_3^- and/or HNO_3 formation in different water matrices as a function of time. Linear regression is used to predict the value of a variable based on the value of another variable. On the other hand, Welch's ANOVA is a statistical test that compares the means of two groups to determine whether they are equal. Unlike classic ANOVA, it can be used when the assumption of homogeneity of variances is violated in the data.

3. Results and Discussion

In the presence of each scavenger, NO_3^-, pH, and conductivity was measured at the beginning, periodically for the first 5 min and then every 15 min, and at the end of the reaction. In addition, at the end of the reactions, escaped ozone, and presence of H_2O_2 were also measured in each case. The O_3 generation capacity of the DBD plasma system used in the experiments was measured as approximately 5 mg O_3/min. The plasma output gas was passed through two serial-connected Drechsel bottle filled with 500 mL of 2% KI solution to capture and measure active species. At the end of the 60 min reaction time, the samples were obtained from each solution and titrated with 0.1 N sodium thiosulfate solution under the reductive condition (the experiments were repeated in three replicates). Since we could not have identified radicals individually in this study, we have tried to make sense of all of them with the oxidative effect of ozone on KI. Figure 2 shows the behavior of NO_3^- and/or HNO_3 formation and escaped ozone in the presence of each scavenger as a summary of the study. The bar KI in Figure 2 is the maximum ozone production of the generator, and this result is given for comparison with other cases.

Our expectation was very simple. If there is no scavenger, the radicals will only tend to form NO_3^- and/or HNO_3, but if there is a scavenger, then the formation will change, and it will decrease. However, our results were not as expected, the findings and possible reasons for the results are explained in the following sections in detail.

3.1. Effect of the Water Matrix on NO_3^- and/or HNO_3 Formation

3.1.1. The Case of Ultrapure Water, Tap Water, and KSW

UPW was obtained from the water purification system and immediately was used in the experiment to prevent the dissolution of carbon dioxide and other interferences. Owing to the absence of the scavenger in the UPW, we expected the highest NO_3^- and/or HNO_3 formation in this experiment, and this experiment was considered to be a control set. At the beginning of the experiments, the pH and conductivity of the UPW were measured as 6.98 (±0.2) and 0.11 µS/cm, respectively. Figure 3a shows the NO_3^- formation when using UPW as the reaction solution, the NO_3^- concentration was increased linearly, and the highest NO_3^- formation was obtained as 357 ± 6.0 mg/L. Tap water and KSW were used in this part of the study as real-water samples. Although in low concentration in both samples, they have a variety of ions and molecules as a scavenger for reactive species,

as explained earlier. The highest NO_3^- formation was obtained in tap water among all cases as 385 ± 4.6 mg/L which contains a wide variety scavenger in low concentration (Figure 3a). This result can be explained by some species in tap water acting as a trap for the radicals. The surface water obtained a relatively low NO_3^- formation of 371 ± 4.9 mg/L, possibly due to the organic carbon content of the KSW. Ozone and other active species may react with organic matter and be consumed by it, so, the nitrate formation chain may be hindered. (The KSW originally contained nitrate 2.43 ± 0.8 mg/L, the initial NO_3^- concentration was subtracted from the obtained concentration when reporting the result).

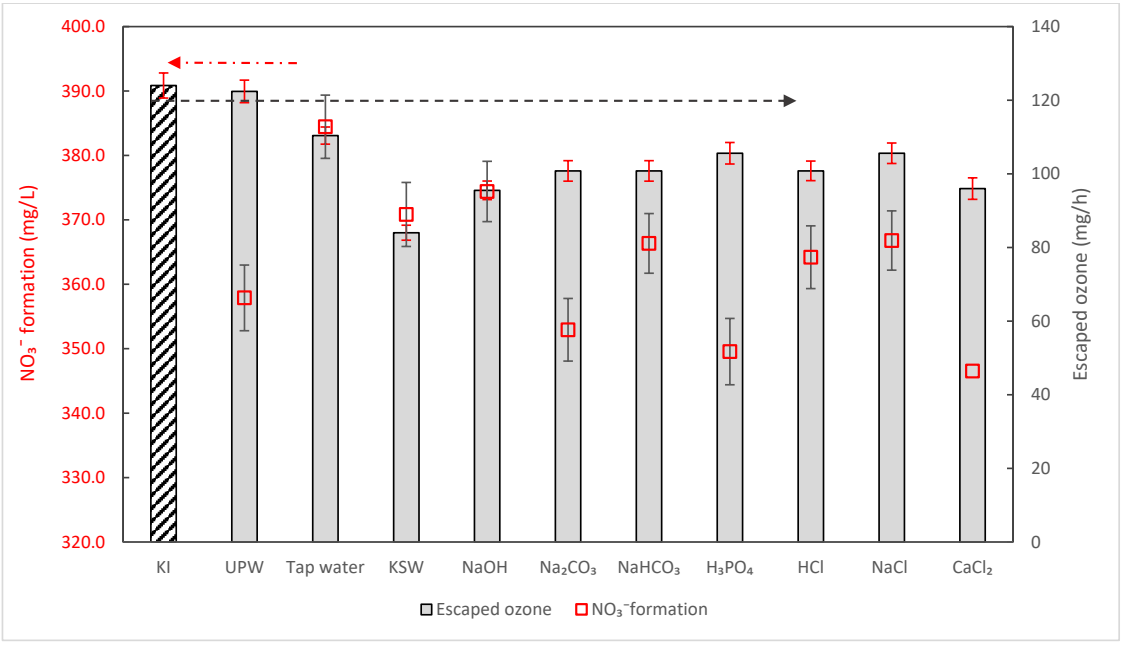

Figure 2. Variation of escaped O_3 and NO_3^- formation as a function of scavengers in the investigated time interval (60 min), the KI bar (▨) is maximum ozone production of the generator, escaped O_3 is given as bars, the NO_3^- formation is given as dots.

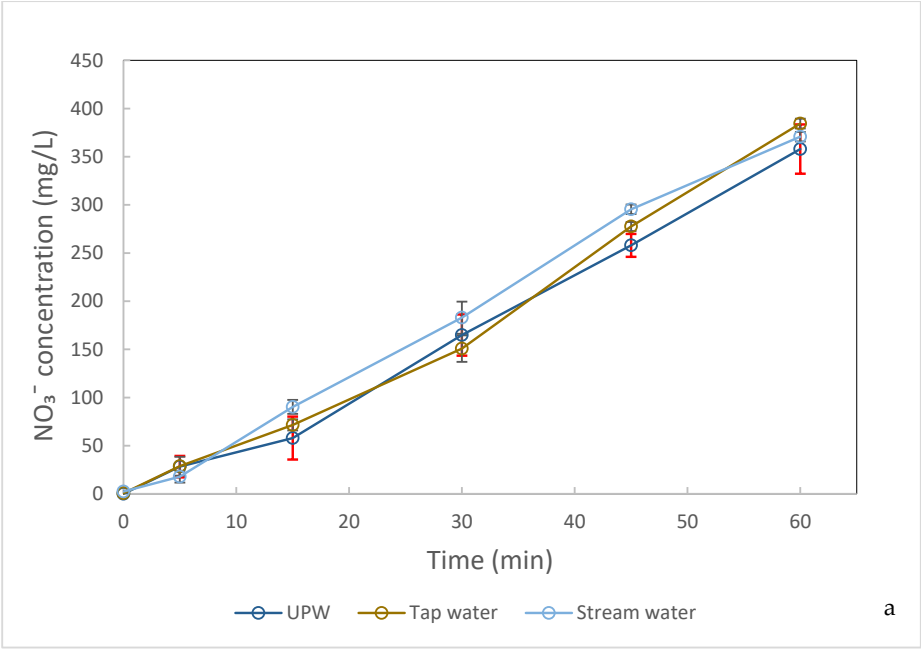

Figure 3. *Cont.*

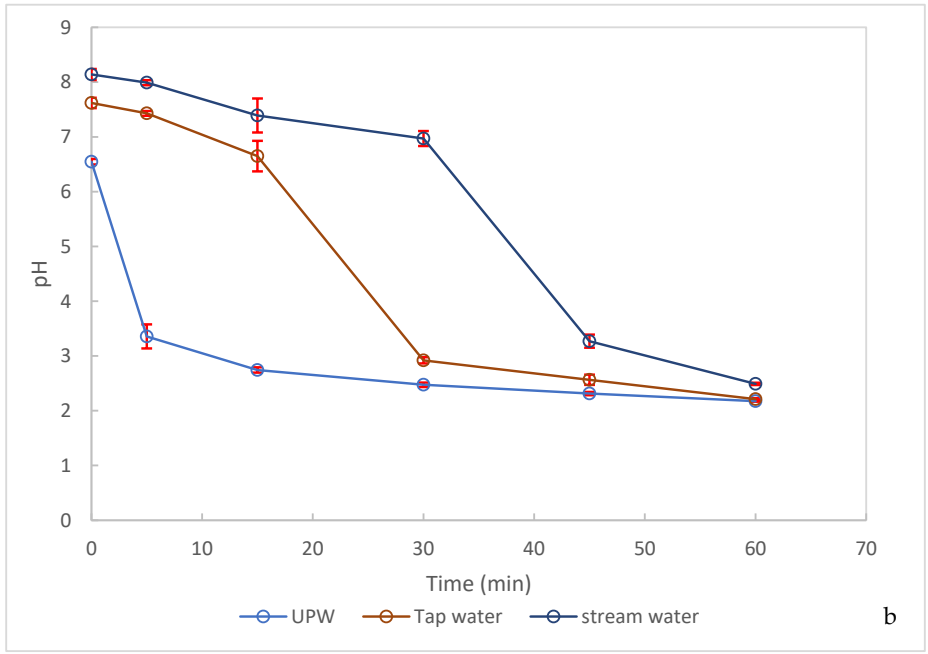

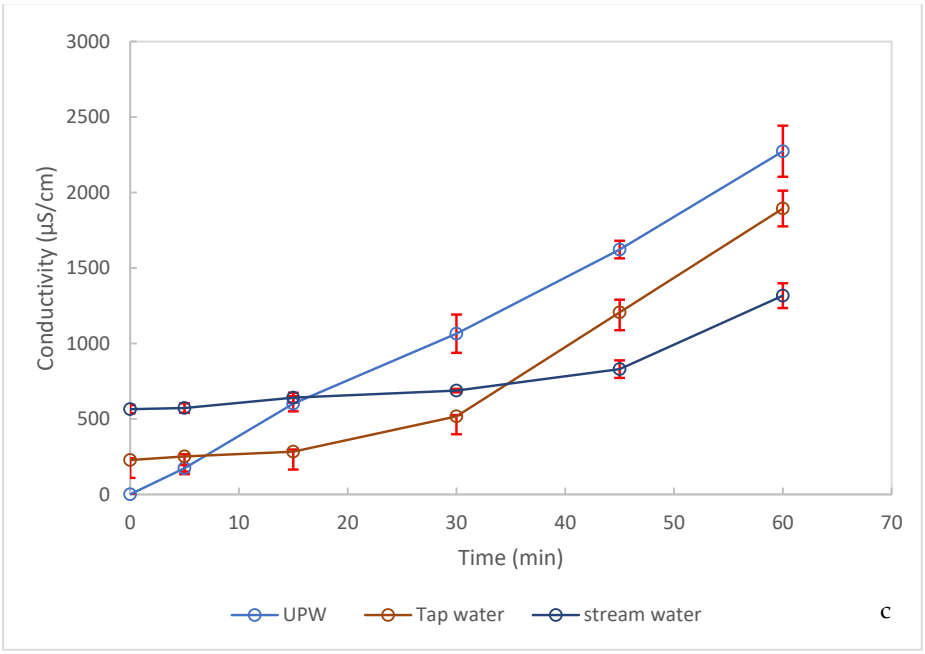

Figure 3. (**a**) Formation of NO_3^- in UPW (without scavengers), tap, and KSW (with scavengers) during plasma-treated gas passes through solutions. (**b**) Change in pH as a function of NO_3^- formation in UPW (without scavengers), tap water, and KSW (with scavengers). (**c**) Change in conductivity as a function of NO_3^- formation in UPW (without scavengers), tap, and KSW (with scavengers).

In the case of the UPW using reaction solution, pH rapidly decreased from 6.98 to 3.37 in five minutes and then decreased slowly to 2.17 at the end of the reaction (Figure 3b). While increasing the NO_3^- formation, decreasing the pH can be explained by the formation of HNO_3. As mentioned in the previous section, some of the radicals are transported to the liquid without being quenched, which provides the precursor for NO_3^- and/or HNO_3 by the reaction between water molecules [3,6,7,16]. Crema et al. studied the degradation of indigo carmine by an NTP system, ozonation with the direct application of plasma, and the post-discharge effect on an aqueous medium. They reported that, at the gas–liquid interface $OH^\bullet$, O and $NO^\bullet$ are formed as intermediates that can remain stable in the water

as NO_3^-, NO_2^-, and H_2O_2 [16]. The pH of tap water and KSW samples decreased from 7.62 to 2.21 and 8.14 to 2.49, respectively, at the end of reaction. In both solutions, the pH was decreased gradually due to the alkalinity of the samples (Figure 3b).

On the other hand, decreasing the pH of the solutions could be due to the intake of CO_2 into the water and the resulting carbonic acid, but it is unlikely in such a short time and does not explain the increase in NO_3^- formation.

The formation of NO_3^- and/or HNO_3 in all solutions caused the ionic strength to increase, and the conductivity of the solution was increased (Figure 3c). The conductivity increase in UPW was linear and at the end of the reaction changed from 0.11 µS/cm to 2200 µS/cm. Due to buffer intensity of the tap water and KSW increasing the conductivity take time, the conductivity change rate increased after the pH of the solutions dropped below the pH neutralization point, and this is detailed in Section 3.1.2.

H_2O_2 formation in UPW was measured periodically, a 0.22 mM H_2O_2 formation was obtained at the 15th min point of the reaction and remained stable until the end of the reaction. The H_2O_2 stability can be explained by the completion of ozone saturation in water and the cyclic ozone formation [17]. On the other hand, with the H_2O_2 formation in KSW, the 15th min point of the reaction was 0.22 mM, then increased by 0.33 mM and remained stable at the end of the reaction, when the case of tap water H_2O_2 formation gradually increased from 0.22 mM to 0.4 mM and remained stable. It can be explained by some impurities such as OH^- ions in the solutions (tap water and KSW) acting as a core for H_2O_2 formation. Unlike our result, Crema et al. reported that with the N_2-NTP application of the water, 1.6×10^{-5} M H_2O_2 formation in the 10th min of the reaction was obtained and then decreased to 1.0×10^{-6} M which remained constant. They explained that the decrease in the H_2O_2 concentration is the decomposition of H_2O_2 into $OH^\bullet$ and/or consumption of H_2O_2 by ozone [16].

Considering that the plasma-treated gas passes through the UPW-containing front vessel before the KI-trap and during the reaction time, it can be said that there are no other radicals in the KI-trap except O_3. In the KI-trap 98.7% of O_3 was present which was very close to when the case KI-trap was being used as a front vessel (Figure 2). In the case of tap water, most of the radicals escaped and 89% of them were trapped in the KI-traps. On the other hand, the highest O_3 consumption occurred when KSW used as reaction solution, in this case 67.7% of O_3, was present in the trap. Since the KSW contains organic carbon and the radicals formed in the plasma reacts without selecting a reactant, this result could be explained by some of the radicals vanishing by reacting with the organic carbon.

3.1.2. The Effect of the Initial OH^- Ion Concentration

As mentioned above, and in light of previous studies stating that the effect of OH^- ion on ozone and NO_3^- and/or HNO_3 formation is different, the difference may have been obtained due to using different plasma sources and reactor configurations. Thus, in the current study, we tried to answer the effect of the OH^- ions on NO_3^- and/or HNO_3 formation in the same experimental condition, except for the liquid phase. For this purpose, 5 mM NaOH, 0.01 N HCl, and 0.01 N H_3PO_4 solutions were used.

Unexpectedly, the second highest NO_3^- concentration was obtained as 379 ± 5.0 mg/L in the highest initial OH^- ion concentration (Figure 4a) among all experimental conditions, even the control set. It can be explained by increasing OH^- ion concentration accelerating the decomposition of O_3 and the formation of increased $OH^\bullet$ radicals [1,8]. With increased $OH^\bullet$ radicals, more chain reactions can occur that lead to the formation of HNO_3. $OH^\bullet$ radicals are involved in HNO_3 formation reactions either directly as a reactant or indirectly as a reactant of HNO_3 precursor and/or isomer formation [3]. As known, $OH^\bullet$ radicals can also provide the formation of H_2O_2 in the water or vice versa [8]. Our results agreed with the previous studies, the highest H_2O_2 formation obtained in the NaOH solution at 0.44 mM at the 15th min point of the reaction remained stable at the end of the reaction.

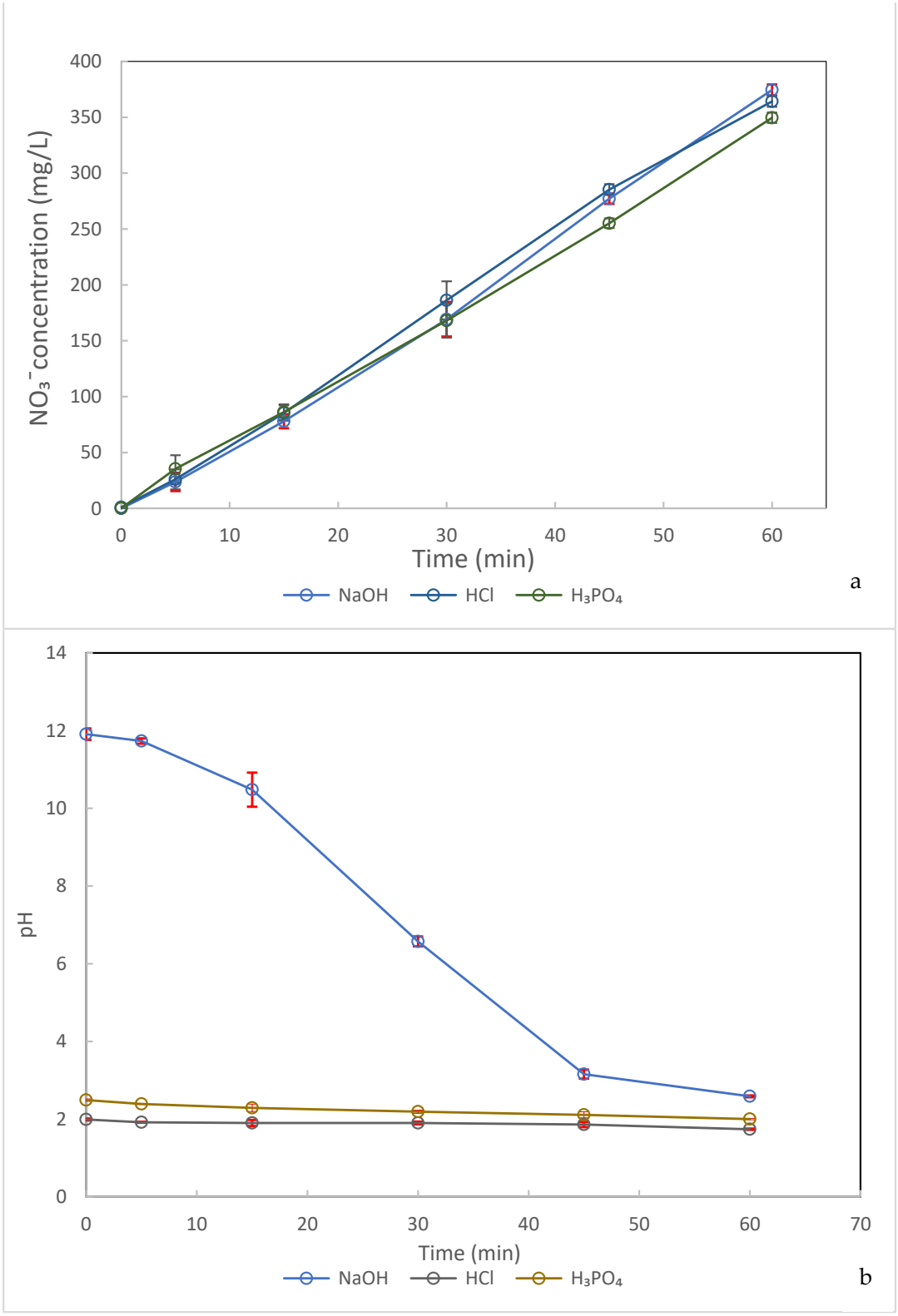

Figure 4. *Cont.*

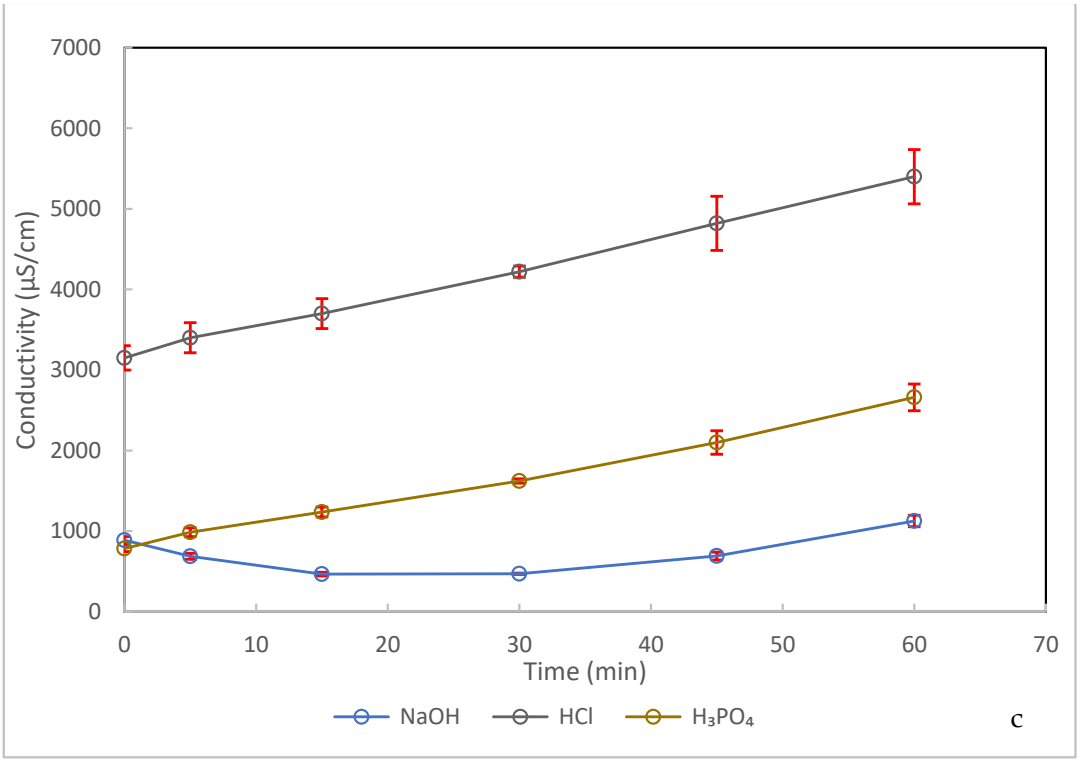

Figure 4. (**a**) The effect of the initial OH^- ion concentration on NO_3^- formation. (**b**) pH changes in 0.01 N HCl, 0.01 N, H_3PO_4, and 5 mM NaOH solutions as different initial OH^- ion concentrations as a function of NO_3^- formation. (**c**) Conductivity changes in 0.01 N HCl, 0.01 N, H_3PO_4, and 5 mM NaOH solutions with different initial OH^- ion concentrations as a function of NO_3^- formation.

In the acidic solutions, NO_3^- concentration was relatively lower than in the alkali solution (Figure 4a). This can be explained by the O_3 stability, as mentioned before the O_3 which is more stable in acidic pH and increasing in the stability of O_3 caused the decrease in $OH^\bullet$ radical formation which was adversely affected by the HNO_3 formation. Especially in the H_3PO_4 solution, we obtained the lowest NO_3^- concentration of 350 ± 4.6 mg/L, which is probably due to H_3PO_4 acting as a scavenger for O_3, and the lack of OH^- ion in the solution hindering the formation of $OH^\bullet$ radicals. The HNO_3 formation, which was determined as 364 + 5.2 mg/L in the HCl solution, was higher than the H_3PO_4 solution.

On the other hand, in both acid solutions, H_2O_2 formation occurred in the same tendency. We observed that within 15 min, a 0.22 mM H_2O_2 formation occurred, followed by an increase to 0.33 mM, remaining stable until the end of the reaction. While the relatively high H_2O_2 formation was expected, the low NO_3^- formation was unexpected. Yet, it could be explained by the fact that in acidic solutions, O_3 is stable, and reactions lead to cyclic ozone formation rather than NO_3^- formation.

On the other hand, Bian et al. studied the effect of the pH on NO_3^- formation using a pulsed high voltage discharge. They reported that increasing the pH of the solution caused the reduced formation of HNO_3 because of the degree conversion of NO_2^- to NO_3^- decreasing at a high pH [4]. However, in our case, NO_2^- formation could not be observed, so we could not comment. Diverse plasma products are generated by distinct plasma sources, as previously stated [6,7].

Based on the result of the experiments, it can be said that the formation and stability of $OH^\bullet$ radicals are very important for NO_3^- and/or HNO_3 formation.

The pH of the NaOH solution decreased gradually from 11.83 to 2.56 as a function of HNO_3 formation (Figure 4b). With the radicals transferred to the solution, HNO_3 is formed instantaneously and reacts with sodium ions to form $NaNO_3$. The experiment HNO_3 formation continued, but due to the inadequate sodium ions in the solution, the

HNO_3 form accumulated instead of $NaNO_3$, which caused a decrease in pH. The buffer capacity of the phosphate near the pK value was high, and in our case, the initial pH of the H_3PO_4 was 2.49, which was so close to pK_1, that the decrease in the pH because of the nitric acid formation was not observed clearly. In the HCl solution, which was a strong acid, the initial pH was very close to the pK value so the decreasing pH because of the HNO_3 formation was not observed clearly, too.

An increase in the ionic strength and the conductivity in the solutions due to the formation of the NO_3^- and/or HNO_3 in the liquid was expected as with those observed in the control experiment. However, in the investigated time interval, the conductivity of the solutions showed different tendencies (Figure 4c). During the experiments, the conductivity of the NaOH solution decreased in 15 min from 890 µS/cm to 460 µS/cm, then increased to 1120 µS/cm (Figure 4c). The change in conductivity can be a result of pH change. As known, there is no direct relation between pH and conductivity but, the solution used in our experiment did not contain any other impurities so we can explain the shifting of conductivity as a function of pH. The conductivity of the solution is lowest when it is close to the neutralization point of the pH, but the conductivity increases farther from the neutralization point. Especially since the mobility of the H^+ ion is almost twice that of the OH^- ion [18], the conductivity increases with increasing H^+ in solution.

Although in the acidic solutions, the pH decreases due to HNO_3 formation cannot be determined clearly, the increase in conductivity linearly is due to the increased H^+ ion concentration in the liquid phase, that is the formation of HNO_3. The conductivity of both HCl and H_3PO_4 solutions showed a similar linear tendency during the investigated time interval.

In the OH^- ion concentration-dominant solution, the second highest O_3 consumption was observed among all cases: 23% of the generated O_3 was consumed. It indicates that if an adequate number of OH^- ions are present, ozone decomposition accelerated, and reacts with RNS to formation of HNO_3. On the other hand, even if O_3 decomposition is accelerated by different scavengers such as H_3PO_4, the HNO_3 formation chain is inhibited if there is inadequate OH^- ion and/or a core. As shown Figure 2 O_3 consumption is more in H_3PO_4 solution than HCl solution but, HNO_3 formation is lower.

3.1.3. The Effect of the Carbonate Species

The carbonate system is one of the important acid–base systems in the water and, the fraction of the inorganic carbon species change is dependent on pH or vice versa. Increasing the total inorganic carbon concentration also provides buffer intensity to the water and is defined as carbonate alkalinity. The carbonate alkalinity adversely affects ozonation and the cyclic ozone chain can be broken [19]. On the other hand, the effect of the carbonate species on NO_3^- and/or HNO_3 formation can be different. Buendia et al. examined various initial $NaHCO_3$ concentrations on NO_3^- formation used by the DBD system above to water surface and reported that the increasing initial alkalinity caused the overall increasing formation rate of NO_3^- to decrease [12]. On the other hand, carbonate (CO_3^{2-}) ions are considered stronger scavengers for $OH^\bullet$ radicals but, the effect of bicarbonate (HCO_3^-) ions on the $OH^\bullet$ radical is neglectable [9].

In this part of the study, we investigate the effect of the ionization fraction of the inorganic carbon species on nitrate formation where 10 mM $NaHCO_3$ and 10 mM Na_2CO_3 solution were used in the experiments, individually. The pH of the $NaHCO_3$ solution was 8.2, which is very close to the HCO_3^- equivalence point, so it was assumed that all inorganic carbon was equal to HCO_3^-. The Na_2CO_3 solution pH was 10.96, where the CO_3^{2-} ion is the dominant species.

In the $NaHCO_3$ solution, the NO_3^- formation was linear at the end of the reaction as 366 ± 4.9 mg/L NO_3^- formation was obtained and, the slope was very close to the control set as UPW (Figure 5a). The result indicated that the HCO_3^- ions are not significantly affected by the NO_3^- formation. Observing that, in the initial CO_3^{2-} ion-dominant solution the NO_3^- formation was insignificantly low at the 30 min point, it is probably due to the

$OH^{\bullet}$ radicals being consumed by the CO_3^{2-}, thus the nitrate formation chain reactions were damaged. Further along in the experiment, with the continued forming of HNO_3 in the solution, CO_3^{2-} ions turned to HCO_3^- ions, and the consumption of the $OH^{\bullet}$ radicals decreased. Thus, the nitrate formation efficiency showed a similar trend to the $NaHCO_3$ solution, and 345 ± 4.6 mg/L of NO_3^- formation was obtained in the solution (Figure 5a).

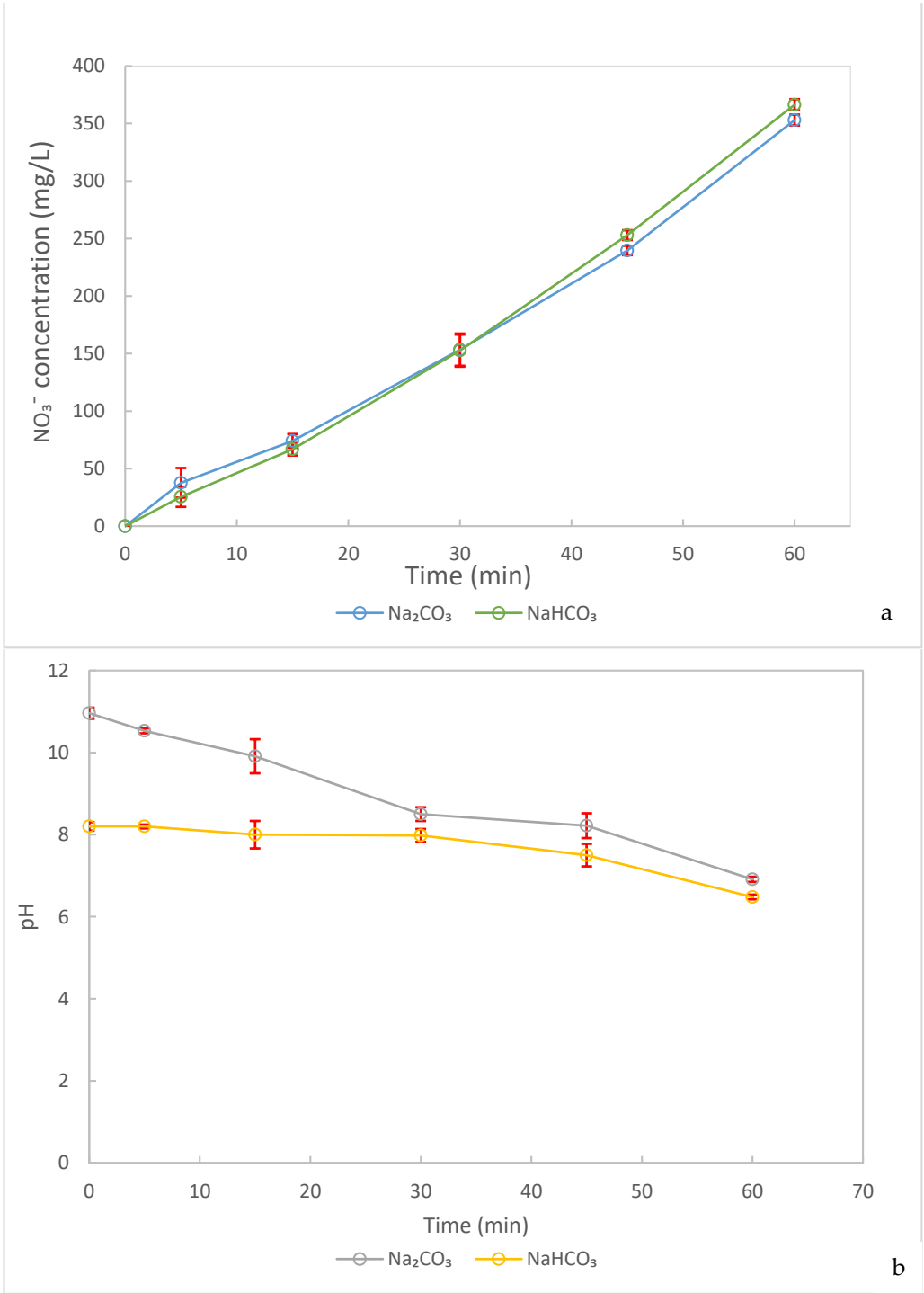

Figure 5. *Cont.*

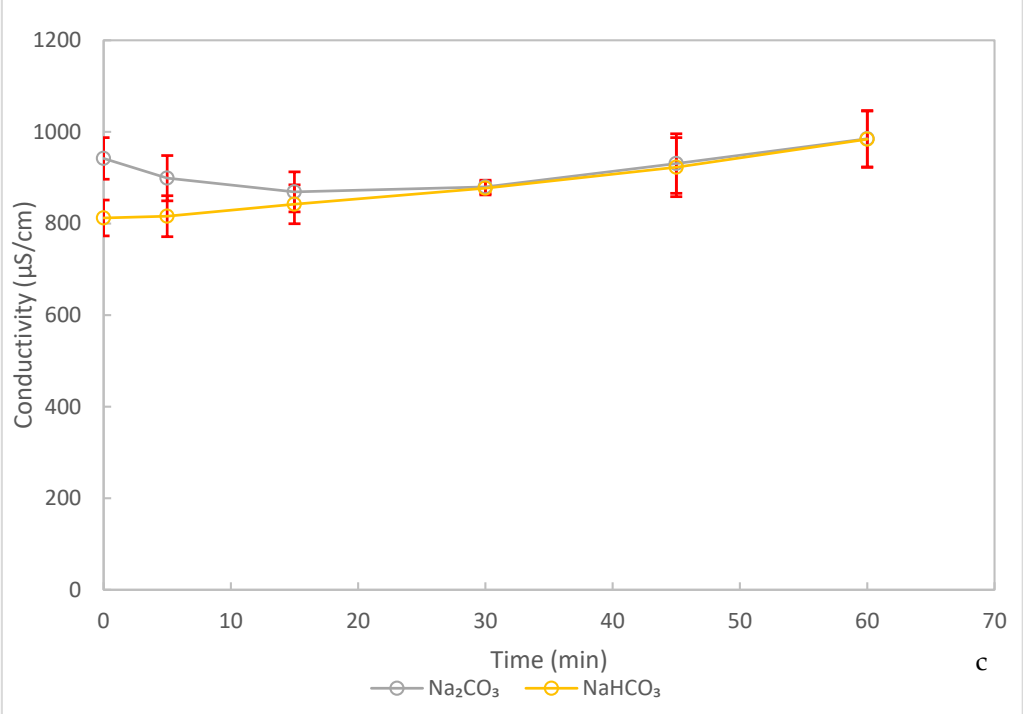

Figure 5. (**a**) The effect of the ionization fraction of the inorganic carbon species on NO_3^- formation, 10 mM $NaHCO_3$, and 10 mM Na_2CO_3. (**b**) pH changes in 10 mM $NaHCO_3$ and 10 mM Na_2CO_3 solutions as a function of NO_3^- formation. (**c**) Conductivity changes in 10 mM $NaHCO_3$ and 10 mM Na_2CO_3 solutions as a function of NO_3^- formation.

The effect of NO_3^- and/or HNO_3 on the pH, in the $NaHCO_3$ solution, was a very slow decrease from 8.2 to 6.48 due to the buffer intensity. On the other hand, the Na_2CO_3 solution showed the pH decreasing relatively remarkably from 10.96 to 8.5 in the 30 min reaction, then slowly decreasing to 6.91 (Figure 5b).

The $NaHCO_3$ solution conductivity relatively increased during the experiment, while the conductivity of the Na_2CO_3 solution slightly decreased from 942 to 869 µS/cm in the first 30 min and then increased to 985 µS/cm. The change in conductivity can be explained by the increased ionic strength of the solutions that was caused by H^+ in the form of HNO_3 (Figure 5c).

The H_2O_2 formation was also affected by the consumption of $OH^\bullet$ radicals; H_2O_2 formation began at a different time duration of the reactions in both carbonate solutions such that the formation of H_2O_2 at 0.22 mM in the $NaHCO_3$ solution was obtained after the 15 min of the reaction, whereas the formation was not observed in the first 30 min of the Na_2CO_3 solution. The H_2O_2 formation in the Na_2CO_3 solution detected in the 45 min reaction was 0.11 mM.

As a result, when it comes to ozone production with DBD, it was seen that the inorganic carbon species had a similar effect on NO_3^- formation and the NO_3^- concentration obtained in both solutions was remarkable.

3.1.4. The Effect of the Ionic Strength

The ionic strength is defined as a function of the charge and concentration of the ions in the liquid; in dilute solutions, the ions behave independently of each other, but with increasing ion concentration, the electrostatic interaction between the ions and intensity of the electric field increase [20]. Thus, discharge of the plasma can be obtained as stable and the HNO_3 formation reaction may increase due to the interaction between ions and radicals.

On the other hand, increasing salt concentration, also known as the salting-out effect, causes a decrease in the solubility of the molecules in the water such as oxygen [20] and

ozone [21]. Gurol and Singer have shown that the ionic strength is effective on the mass-transfer coefficient of O_3 by changing the interfacial area of the bubbles, increasing the ionic strength caused by the decreasing solubility and the accelerated decomposition rate of O_3 in the water [21]. So, O_3, which is one of the reactive oxygen species, is affected by ionic strength; we therefore investigated the answer to the question of whether the other reactive species that are effective in the formation of NO_3^- and/or HNO_3 are affected by ionic strength. Thus, two brine solutions were prepared using NaCl and $CaCl_2$ which have the same ionic strengths (μ) as 0.7 M. To reach the same ionic strength, 42 g of NaCl and 25.9 g of $CaCl_2$ per liter were added in each solution; the pH and conductivity of the solutions were 6.45 and 5.76, and 56.3 mS/cm and 29.8 mS/cm, respectively.

Obtaining the NO_3^- concentration in NaCl solution was 367 ± 4.8 mg/L, and 346 ± 4.6 mg/L in the $CaCl_2$ solution (Figure 6a). When the results of the experiments with the same ionic strength but different salts are compared with the control experiment, it can be said that obtaining NO_3^- formation is low, because of the salting-out effect of the solution. However, if we compare the salts among themselves, the solutions either increase their conductivity or the chlorine (Cl^-) concentration has a positive effect on the formation of NO_3^-. Razumovskii et.al. showed that the Cl^- accelerated the decomposition rate of ozone, thus O_3^- could be formed in water. The O_3^- formation could be increased by $OH^\bullet$ and increasing $OH^\bullet$ could be promoted by chain reactions to form HNO_3 [22].

The pH of both solutions decreased sharply in the 5 min for the NaCl solution from 6.45 to 3.09, from 5.76 to 2.8 for the $CaCl_2$ solution, then progressively decreased and, the conductivity of both solutions relatively increased (Figure 6b). Due to the high conductivity of the solutions, the conductivity could not be measured sensitively.

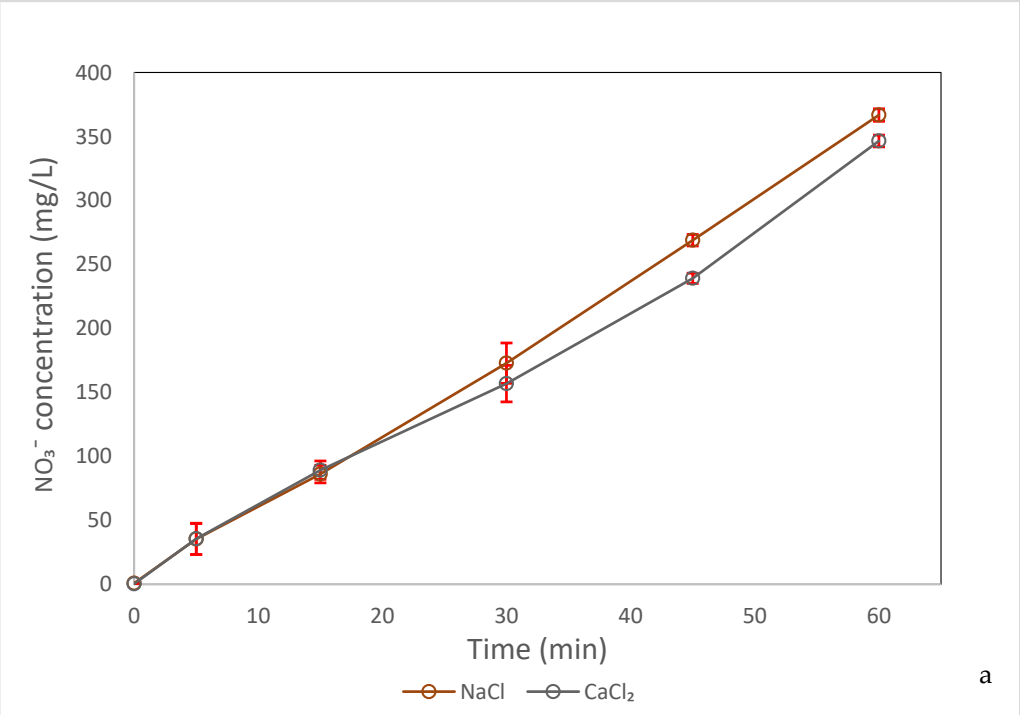

Figure 6. *Cont.*

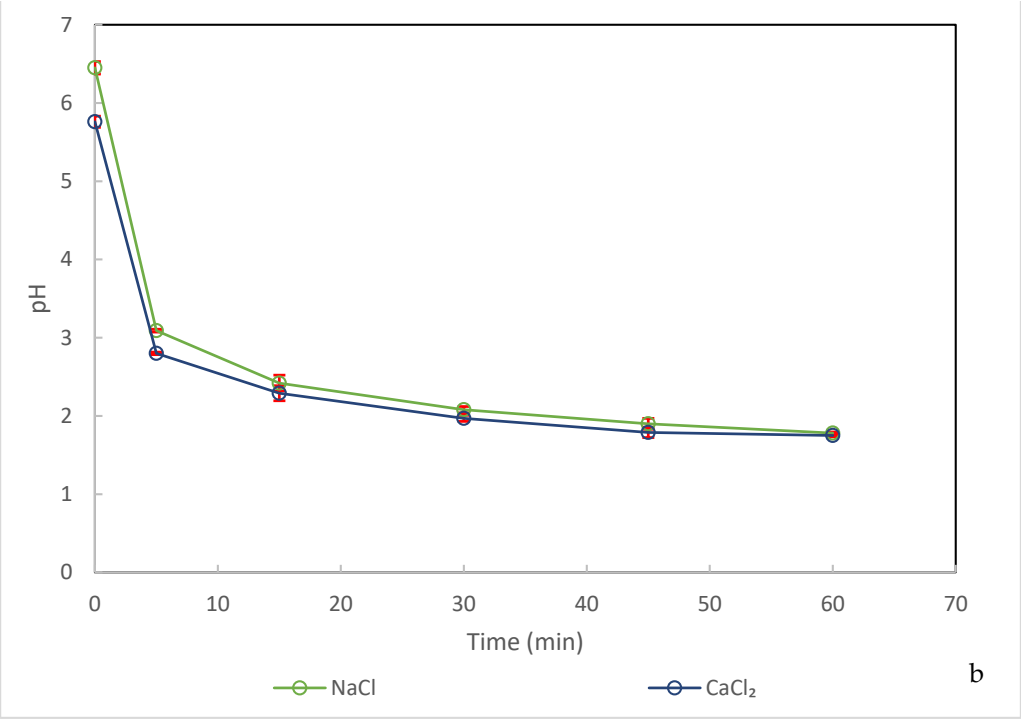

Figure 6. (**a**) The effect of the initial ionic strength on NO_3^- formation. (**b**) The effect of the ionic strength of the solution species on pH.

3.1.5. The Effect of the Ionic Strength

The statistical data of linear regression is presented in Table 3. Furthermore, the ANOVA results for linear regression, the statistical Welch's test results for nitrate concentrations in the presence of different scavengers at the initial condition, Games-Howell Pairwise Comparisons obtained from the One-Way Welch's ANOVA for nitrate concentrations in the presence of different scavengers at the initial condition, the statistical Welch's test results for nitrate formations in the presence of different scavengers at the final condition, Games-Howell Pairwise Comparisons obtained from the One-Way Welch's ANOVA for nitrate formations in the presence of different scavengers at the final condition are presented in Tables S1–S5, respectively.

Table 3. The statistical data of linear regression.

	Intercept	Intercept	Slope	Slope	Statistics	Intercept	Slope
	Value	Standard Error	Value	Standard Error	Adj. R-Square	*t*-Value	*t*-Value
UPW	−10.683	8.72179	6.00645	0.25955	0.99073	−1.22486	23.14149
Tap	−12.6739	11.9088	6.38587	0.3544	0.98479	−1.06424	18.01903
KSW	−4.91477	6.17878	6.38175	0.18388	0.99586	−0.79543	34.70693
NaOH	−9.11918	5.45704	6.30462	0.1624	0.99669	−1.67109	38.82224
Na_2CO_3	−3.41312	9.1083	5.66663	0.27106	0.98866	−0.37473	20.90578
$NaHCO_3$	−12.0936	9.64839	6.04389	0.28713	0.98882	−1.25344	21.04944
H_3PO_4	1.23393	3.09508	5.72337	0.09211	0.99871	0.39868	62.13813
HCl	−2.29049	4.00673	6.20551	0.11924	0.99816	−0.57166	52.04348
NaCl	−0.64245	3.78247	6.0316	0.11256	0.99826	−0.16985	53.58407
$CaCl_2$	1.39872	6.9549	5.54413	0.20697	0.99307	0.20111	26.78682

The high values of the adjusted R-square (<0.984) indicate a nearly linear increase across all matrices. The slope values presented in Table 3 also give information about the overall NO_3^- production rate. The higher slope values obtained for tap water and KSW (~6.38) prove the presence of some species acting as a trap and/or core for NO_3^- formation. Another higher slope value was determined for NaOH (~6.30) potentially due to the initial

high OH^- ion concentration leading to the decomposition of ozone. The reason for the lower slope values obtained for Na_2CO_3 and H_3PO_4 (~5.66 and ~5.72, respectively) can be explained by the presence of carbonate and phosphoric acid acting as scavengers for $OH^•$ radicals. For chloride salts, the slope values were also determined to be lower due to the salting-out effect. Lastly, the absence of scavengers in UPW negatively affects the NO_3^- -forming chain reactions leading to the relatively low slope value (~6.00).

Welch's ANOVA test results and Games–Howell Pairwise Comparison table for NO_3^- concentrations at initial and final conditions at 60th minutes as a function of scavengers are given in Tables S2–S5.

In the comparison table, the *p*-values higher than 0.05 (below 95% confidence level) are an indication of non-similarity between scavengers. At the initial condition, the most dissimilarity was obtained for the $CaCl_2$-tap water (1.00), Na_2CO_3-NaOH (0.75), $CaCl_2$-$NaHCO_3$ (0.74), and $CaCl_2$-NaOH (0.72) comparisons with the *p*-values above 0.70; while the most similarity was obtained for HCl-NaOH (5.2×10^{-4}), NaCl-NaOH (7.6×10^{-4}), KSW-tap water (7.0×10^{-3}), and NaOH-tap water (4.8×10^{-3}) with the *p*-values below 0.01.

At the final condition at 60 min, significant comparisons were obtained for NaCl-HCl (8.1×10^{-4}), HCl-H_3PO_4 (2.0×10^{-5}), NaCl-H_3PO_4 (1.7×10^{-5}), Na_2CO_3-tap water (0.01), H_3PO_4-tap water (0.01), HCl-tap water (0.02), and NaCl-tap water (0.02). The marginal media were determined as UPW and $CaCl_2$ (*p*-value: 1.0). The comparisons of all scavengers with $CaCl_2$, $NaHCO_3$, UPW, and KSW were non-significant. Moreover, the only significant dual comparison for Na_2CO_3 was obtained with tap water. As a result of statistical analysis, the number of significant dual comparisons are more at the initial condition than the final condition due to the closer initial nitrate concentrations than the final concentrations, because the aqueous phase of scavengers was prepared synthetically in UPW by using analytical grade chemicals except for KSW and tap water.

During the investigated time intervals, some radicals were quenched by scavengers, and therefore nitrate formation chain reactions were adversely affected leading to a decrease in nitrate formation. Individually, the salting-out effect of chloride salts (1), the presence of carbonates (2), the organic carbon content in KSW (3), and the absence of core and/or trap in UPW (4) led to non-significant results.

4. Conclusions

In this study, we compared the scavenging activities of common scavengers on NO_3^- and/or HNO_3 formation when using the DBD system fed with ambient air. Based on the results, it can be said that scavenger concentration is more effective than increasing the diversity of scavengers in the water, and NO_3^- and/or HNO_3 formation is adversely affected by both increasing scavenger concentration and the absence of scavengers. The highest NO_3^- formation was obtained in the tap water as 385 ± 4.6 mg/L while the lowest NO_3^- formation was 347 ± 4.7 mg/L in $CaCl_2$ solution. The remarkable NO_3^- formation obtained in all water samples showed that the DBD system could be beneficial for irrigation after pH adjustment, depending on the soil and the type of plant to be grown.

On the other hand, we obtained notable nitrate concentration at the end of the experiments in all cases. The results showed that the water matrix is relatively effective on NO_3^- and/or HNO_3 formation when using the DBD system fed with ambient air. Moreover, previous studies demonstrated that NO_3^- formation occurred in the liquid phase even using N_2 as feed gas, as a function of long-lived species, and/or interaction between plasma-treated gas and water [7,17]. When NTP systems are intended to be used for water/wastewater treatment, it should be considered that nitrate will be formed in the liquid phase. This means the inclusion of a compound "NO_3^-" is needed by various microorganisms in the liquid phase and thus contamination is increased. In addition, it has been revealed in many studies that nitrate in drinking water will create various health problems if consumed [23–26].

Lastly, the production of NO_3^- and/or HNO_3 with an NTP system may be considered "not feasible" today because it has many obstacles in technical and economic aspects.

However, we believe that with the optimization of the system configuration, NTP will be accepted as a new nitrate-based compound and/or nitric acid production method soon. In the current study, we kept the DBD system and environmental conditions constant to avoid their effects on NO_3^- and/or HNO_3 formation. Our further study will be to examine different plasma sources and plasma creation variability on NO_3^- and/or HNO_3 formation.

Supplementary Materials: The following supporting information can be downloaded at: https://www.mdpi.com/article/10.3390/w15101840/s1, Table S1: The ANOVA results for linear regression. Table S2. The statistical Welch's test results for nitrate concentrations in the presence of different scavengers at the initial condition. Table S3. Games-Howell Pairwise Comparisons obtained from the One-Way Welch's ANOVA for nitrate concentrations in the presence of different scavengers at the initial condition. Table S4. The statistical Welch's test results for nitrate formations in the presence of different scavengers at the final condition. Table S5. Games-Howell Pairwise Comparisons obtained from the One-Way Welch's ANOVA for nitrate formations in the presence of different scavengers at the final condition.

Author Contributions: Writing—original draft preparation, U.D.K.-S. and T.Y.; writing—review and editing, U.D.K.-S. and T.Y. All authors have read and agreed to the published version of the manuscript.

Funding: This study is part of a research project (Grant No. 122Y089) financially supported by the Scientific and Technological Research Council of Turkey (TUBITAK).

Data Availability Statement: Not applicable.

Conflicts of Interest: The authors declare no conflict of interest.

References

1. Heidt, L.J.; Landi, V.R. Ozone and Ozonide Production and Stabilization in Water. *J. Chem. Phys.* **1964**, *41*, 176–178. [CrossRef]
2. Atkinson, R.; Baulch, D.L.; Cox, R.A.; Crowley, J.N.; Hampson, R.F.; Hynes, R.G.; Jenkin, M.E.; Rossi, M.J.; Troe, J. Evaluated Kinetic and Photochemical Data for Atmospheric Chemistry: Volume I-Gas Phase Reactions of O_x, HO_x, NO_x and SO_x Species. *Atmos. Chem. Phys.* **2004**, *4*, 1461–1738. [CrossRef]
3. Oehmigen, K.; Winter, J.; Hähnel, M.; Wilke, C.; Brandenburg, R.; Weltmann, K.D.; Von Woedtke, T. Estimation of Possible Mechanisms of *Escherichia coli* Inactivation by Plasma Treated Sodium Chloride Solution. *Plasma Process. Polym.* **2011**, *8*, 904–913. [CrossRef]
4. Bian, W.; Song, X.; Shi, J.; Yin, X. Nitrogen Fixed into HNO3 by Pulsed High Voltage Discharge. *J. Electrost.* **2012**, *70*, 317–326. [CrossRef]
5. Lin, F.; Wang, Z.; Ma, Q.; He, Y.; Whiddon, R.; Zhu, Y.; Liu, J. N2O5 Formation Mechanism during the Ozone-Based Low-Temperature Oxidation DeNOx Process. *Energy Fuels* **2016**, *30*, 5101–5107. [CrossRef]
6. Lukes, P.; Dolezalova, E.; Sisrova, I.; Clupek, M. Aqueous-Phase Chemistry and Bactericidal Effects from an Air Discharge Plasma in Contact with Water: Evidence for the Formation of Peroxynitrite through a Pseudo-Second-Order Post-Discharge Reaction of H_2O_2 and HNO_2. *Plasma Sources Sci. Technol.* **2014**, *23*, 015019. [CrossRef]
7. Takahashi, K.; Satoh, K.; Itoh, H.; Kawaguchi, H.; Timoshkin, I.; Given, M.; Macgregor, S. Production Characteristics of Reactive Oxygen/Nitrogen Species in Water Using Atmospheric Pressure Discharge Plasmas. *Jpn. J. Appl. Phys.* **2016**, *55*, 07LF01. [CrossRef]
8. Hoigné, J.; Bader, H. The Role of Hydroxyl Radical Reactions in Ozonation Processes in Aqueous Solutions. *Water Res.* **1976**, *10*, 377–386. [CrossRef]
9. Von Gunten, U. Ozonation of Drinking Water: Part I. *Oxidation Kinetics and Product Formation. Water Res.* **2003**, *37*, 1443–1467. [PubMed]
10. Gardoni, D.; Vailati, A.; Canziani, R. Decay of Ozone in Water: A Review. *Ozone Sci. Eng.* **2012**, *34*, 233–242. [CrossRef]
11. Brisset, J.L.; Pawlat, J. Chemical Effects of Air Plasma Species on Aqueous Solutes in Direct and Delayed Exposure Modes: Discharge, Post-Discharge and Plasma Activated Water. *Plasma Chem. Plasma Process.* **2016**, *36*, 355–381. [CrossRef]
12. Buendia, J.A.; Perez-Lopez, E.; Venkattraman, A. System-Level Model and Experiments for Irrigation Water Alkalinity Reduction and Enrichment Using an Atmospheric Pressure Dielectric Barrier Discharge. *Water Res.* **2018**, *144*, 728–739. [CrossRef] [PubMed]
13. Yoon, S.Y.; Yi, C.; Eom, S.; Park, S.; Kim, S.B.; Ryu, S.; Yoo, S.J. Effects of Gas Temperature in the Plasma Layer on RONS Generation in Array-Type Dielectric Barrier Discharge at Atmospheric Pressure. *Phys. Plasmas* **2017**, *24*, 123516. [CrossRef]
14. Clesceri, L.S.; Greenberg, A.E.; Eaton, A.D. *Standard Methods for the Examination of Water and Wastewater*, 12th ed.; American Public Health Associattion: Washington, DC, USA, 1998.
15. Furman, H.N.; Wallace, J.H. Applications of Ceric Sulfate in Volumetric Analysis. VI. Oxidation of Hydrogen Peroxide by Ceric Sulfate. Indirect Determination of Lead. *J. Am. Chem. Soc.* **1929**, *51*, 1449–1453. [CrossRef]

16. Crema, A.P.S.; Piazza Borges, L.D.; Micke, G.A.; Debacher, N.A. Degradation of Indigo Carmine in Water Induced by Non-Thermal Plasma, Ozone and Hydrogen Peroxide: A Comparative Study and by-Product Identification. *Chemosphere* **2020**, *244*, 125502. [CrossRef]
17. Glaze, W.H. Drinking-Water Treatment with Ozone Ozone Is a Powerful Disinfectant and Oxidant, but Its Chemical Byproducts Need to Be Better Understood. *Environ. Sci. Technol.* **1987**, *21*, 224–230. [CrossRef]
18. Lee, S.H.; Rasaiah, J.C. Proton Transfer and the Mobilities of the H+ and OH− Ions from Studies of a Dissociating Model for Water. *J. Chem. Phys.* **2011**, *135*, 124505. [CrossRef]
19. Mizuno, T.; Tsuno, H.; Yamada, H. Effect of Inorganic Carbon on Ozone Self-Decomposition. *Ozone Sci. Eng.* **2007**, *29*, 31–40. [CrossRef]
20. Snoyeink, V.L.; Jenkins, D. *Water Chemistry*; Wiley: New York, NY, USA, 1980; ISBN 9780471051961.
21. Gurol, M.D.; Singer, P.C. Kinetics of Ozone Decomposition: A Dynamic Approach. *Environ. Sci. Technol.* **1982**, *16*, 377–383. [CrossRef] [PubMed]
22. Razumovskii, S.D.; Konstantinova, M.L.; Grinevich, T.V.; Korovina, G.V.; Zaitsev, V.Y. Mechanism and Kinetics of the Reaction of Ozone with Sodium Chloride in Aqueous Solutions. *Kinet. Catal.* **2010**, *51*, 492–496. [CrossRef]
23. Orbuleț, O.D.; Dăncilă, A.M.; Căprărescu, S.; Modrogan, C.; Purcar, V. Nitrates Removal from Simulated Groundwater Using Nano Zerovalent Iron Supported by Polystyrenic Gel. *Polymers* **2023**, *15*, 61. [CrossRef] [PubMed]
24. Breida, M.; Younssi, S.A.; Bouazizi, A.; Achiou, B.; Ouammou, M.; Rhazi, M. El Nitrate Removal from Aqueous Solutions by γ-Al_2O_3 Ultrafiltration Membranes. *Heliyon* **2018**, *4*, 498. [CrossRef] [PubMed]
25. Nadin, J. Are the Current Methods of Remediation to Reduce Nitrate Contamination in Groundwater in the Developing World Effective? A Systematic Review. *Plymouth Stud. Sci.* **2014**, *7*, 118–150.
26. Mohseni-Bandpi, A.; Elliott, D.J.; Zazouli, M.A. Biological Nitrate Removal Processes from Drinking Water Supply—A Review. *J. Environ. Health Sci. Eng.* **2013**, *11*, 35. [CrossRef] [PubMed]